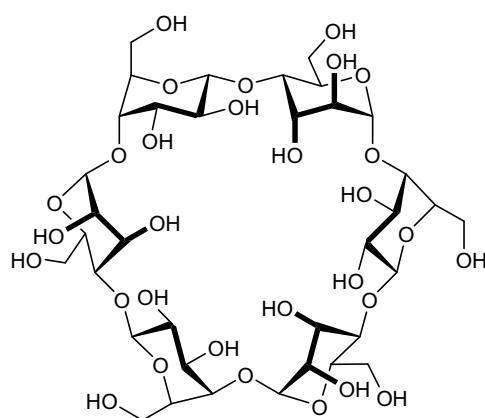


Chapter 3

α -Cycloaltrin



Synthesis, Structure, and Conformational Features of α -Cycloaltrin: a Cyclooligosaccharide with alternating 4C_1 and 1C_4 Pyranose Chairs

Y. Nogami, K. Nasu, T. Koga, K. Ohta, K. Fujita, S. Immel, H. J. Lindner, G. E. Schmitt, and F. W. Lichtenthaler,
Angew. Chem. **1997**, *109*, 1987-1991; *Angew. Chem. Int. Ed. Engl.* **1997**, *35*, 1899-1902.

Solution Geometries and Lipophilicity Patterns of α -Cycloaltrin

S. Immel, K. Fujita, and F. W. Lichtenthaler,
Chem. Eur. J. **1999**, *5*, 3185-3192.

Inclusion Complexes of Cycloaltrins

S. Immel, K. L. Larsen,
unpublished results.

Synthesis, Structure, and Conformational Features of α -Cycloaltrin: A Cyclooligosaccharide with Alternating ${}^4C_1/{}^1C_4$ Pyranoid Chairs**

Yasuyoshi Nogami, Kyoko Nasu, Toshitaka Koga, Kazuko Ohta, Kahee Fujita,* Stefan Immel, Hans J. Lindner, Guido E. Schmitt, and Frieder W. Lichtenthaler*

The wealth of knowledge that has accumulated on the starch-derived cyclodextrins and their unique ability to form inclusion complexes^[1] is contrasted by a peculiar paucity of data on cyclooligosaccharides composed of sugars other than glucose.^[2] Except for certain cyclofructins, obtainable by bacterial action on the polysaccharide inulin,^[3] all of the non-glucose cyclooligosaccharides presently known have been acquired synthetically and require laborious multistep procedures to assemble the linear oligosaccharide from its monosaccharide units in a form suitable for cycloglycosylation. In this way, α (1 \rightarrow 4)-linked cyclooligosaccharides composed of D-mannose^[4] (α -, β -, and γ -cyclomannin), of L-rhamnose^[5] (α -cyclorhamnin), and of alternating D-mannose/L-rhamnose units^[6] have been prepared, yet in such minute amounts as to preclude investigations into their inclusion complex behavior. Molecular modeling studies on α -cyclomannin^[7] and its 6-deoxy L-analogue α -cyclorhamnin^[2] showed that their axially disposed 2-OH points away from the cavity; thus they fairly closely resemble α -cyclodextrin in backbone structure, cavity dimensions, and lipophilicity patterns. The same, in fact, is to be expected for the cyclohexasaccharide with alternating D-mannose and L-rhamnose units. For a cyclogalactin composed of six β (1 \rightarrow 4)-linked galactopyranose residues, molecular modeling revealed an α -CD-like geometry, yet a distinctly different lipophilicity distribution such that hydrophobic surface regions at the primary hydroxyl face are substantially enlarged.^[7]

More profound changes in shape, cavity dimensions, and guest binding properties are to be anticipated for cyclooligosaccharides with axially disposed 3-OH groups in the pyranoid rings— α -cycloaltrin for example—as these would be directed towards the interior of the cavity, resulting in considerable steric congestion, which is likely to be released by deformation of the 4C_1 chairs. Topologically even more interesting appears to be α -cycloaltrin, as the 4C_1 and 1C_4 conformations of α -altropyranoid chairs are very similar in stability^[8] and, hence, in a macrocyclic array several conformations could be formed, such as the all- 4C_1 (**1a**) or all- 1C_4 forms (**1b**), or even more likely in solution, an equilibrium between the two, that passes through the skew 0S_2 geometries (**1c**) of the pyranoid rings (Scheme 1).

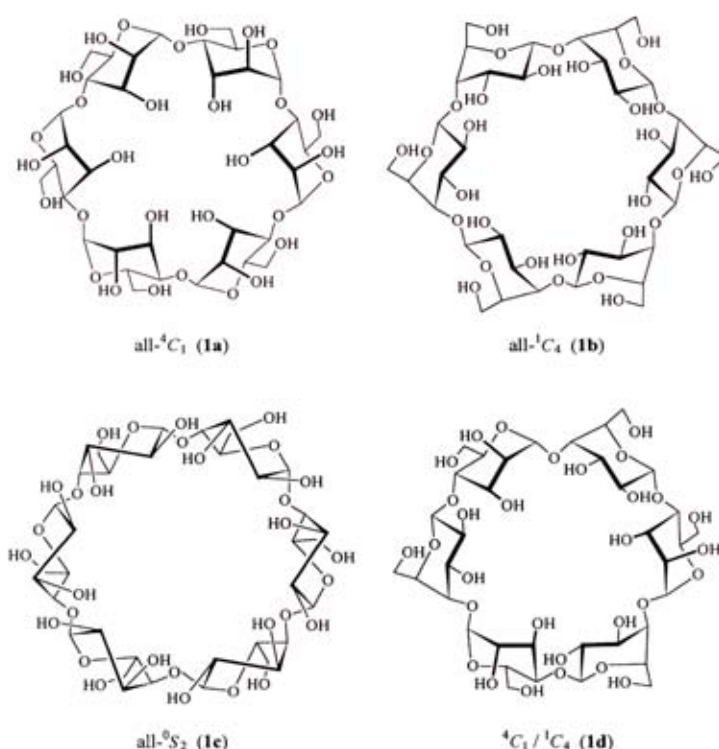
In context with our studies on non-glucose cyclooligosaccharides,^[2] we report on a straightforward synthesis of α -cycloaltrin

[*] Prof. K. Fujita, K. Ohta
Faculty of Pharmaceutical Sciences
Nagasaki University
Nagasaki 852 (Japan)
Fax: Int. code + (958)46-5736

Prof. Dr. F. W. Lichtenthaler, Dr. S. Immel, Prof. Dr. H. J. Lindner, Dipl.-Ing. G. E. Schmitt
Institut für Organische Chemie der Technischen Hochschule
D-64287 Darmstadt (Germany)
Fax: Int. code + (6151)16-6674

Prof. Y. Nogami, K. Nasu, Prof. T. Koga
Daiichi College of Pharmaceutical Sciences, Fukuoka 815 (Japan)
Fax: Int. code + (925)53-5698

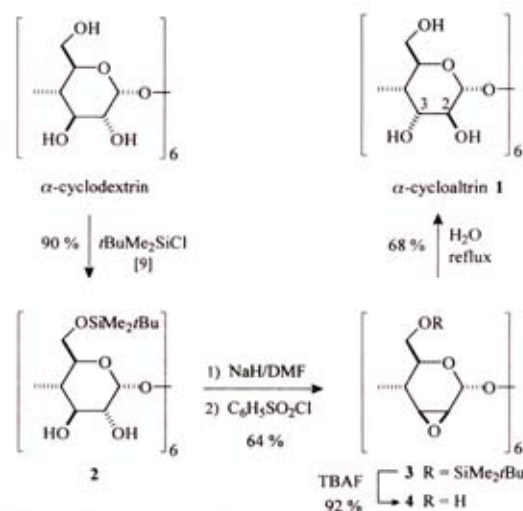
[**] Molecular Modeling of Saccharides, Part 15. This work was supported by the Fonds der Chemischen Industrie and the Nihon Shokuhin Kako (Japan Maize Products Co.). Part 14: Ref. [2]



Scheme 1. Molecular geometries for α -cycloaltrin (**I**), a cyclooligosaccharide composed of six α (1 \rightarrow 4)-linked D-altropyranose residues. In aqueous solution, a dynamic equilibrium prevails between forms **1a–1c**, and various other intermediate conformations; in the solid state, the structure is that of **1d**, comprising a unique alternating sequence of 4C_1 and 1C_4 altropyranoid chair forms.

(**I**) from α -cyclodextrin its molecular geometries in the solid state, revealing a unique alternating sequence of 4C_1 and 1C_4 chairs (**1d**), and in solution, in which a dynamic equilibrium of the type **1a** \rightleftharpoons **1c** \rightleftharpoons **1d** prevails.

The conversion of α -cyclodextrin into **I** started with protection of the six primary hydroxyl groups by the *tert*-butyldimethylsilyl moiety (\rightarrow **2**^[9]). Ensuing deprotonation of the secondary hydroxyls in **2** by treatment with NaH in DMF was followed by the addition of benzenesulfonyl chloride, which not only effected selective 2-*O*-sulfonylation but, concomitantly, displacement of the 2-sulfonyloxy group by the vicinal 3-OH to elaborate the key intermediate, the 6-*O*-protected 2,3-anhydro- α -cyclomannin (**3**, 64%). Deblocking with TBAF/THF yielded



Scheme 2. Synthesis of **I** from α -cyclodextrin.

COMMUNICATIONS

4 (92%), which simply by refluxing in water was converted into **1** and isolated by reversed-phase chromatography (68%). The overall yield for the four-step sequence is a satisfactory 36%, but is lower than the conversion of β -cyclodextrin into its all-*altro* analogue (52%^[10]), obviously reflecting the lesser steric strain, and hence cleaner reactions, in the cycloheptamer.

Cyclomaltrin **1** crystallized with 21 water molecules and is thus embedded in a water matrix in the solid state. Its X-ray structural analysis^[11] not only gave evidence of the water molecules built into the crystal lattice (Figure 1), but revealed the unique

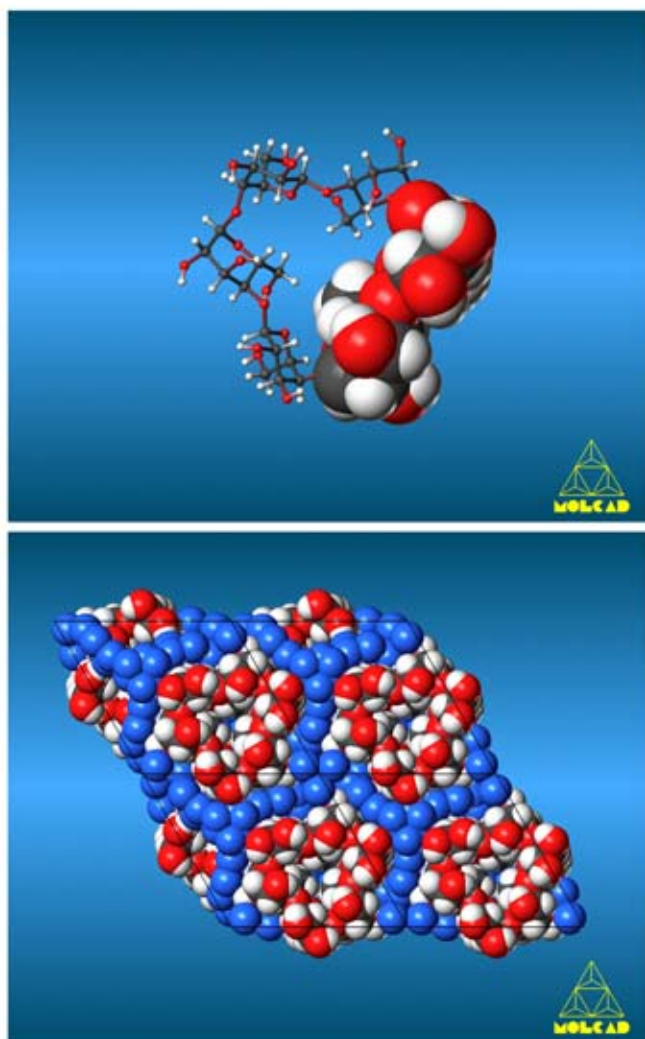


Figure 1. Structure of cyclomaltrin (α -cycloaltrin, **1**) [12]. Top: Ball-and-stick model of the alternating sequence of 4C_1 and 1C_4 chair conformations of altropyranoid rings; in this way the macrocycle is constructed from three banana-shaped disaccharide units, one of which is depicted in a space-filling representation. Bottom: The macrocycle has a compact, disklike topology, devoid of a cavity and is embedded in a water matrix (**1** · 21 H_2O); the disks are stacked in offset layers.

conformational features of the altropyranoid rings: neither the all- 4C_1 form **1a** or the all- 1C_4 form **1b** is adopted, nor one of the various nonchair conformations conceivable (for instance, **1c**); instead, the altrose units display alternate 4C_1 and 1C_4 altropyranoid chair conformations (Figure 1, top), entailing the macrocycle to be made up of three banana-shaped disaccharide portions. The molecules are disk-shaped, devoid of a cavity, and stacked in transposed layers (Figure 1, bottom), the space in between being occupied by water molecules.

The closeness of the chair conformations to the ideal is remarkable: nearly perfect geometry in the 1C_4 -portions with O_4 and C_6 in a fairly antiparallel disposition (167.5°) and with the six pyranoid ring torsion angles in the 52 – 58° range. The 4C_1 chairs, by contrast, are less ideal, as the C_1 - C_2 - C_3 - C_4 torsion angle (-45.7°) reveals some flattening at C-2 and C-3, whilst O_1 , O_2 , and O_3 are still in a fairly antiparallel disposition (O_1 - C_1 - C_2 - O_2 166.2° , O_2 - C_2 - C_3 - O_3 166.5°). Another salient feature of the structure is the different orientations of the 6-OH groups relative to the pyranoid rings: *gauche*-*trans* disposition ($\omega = 55.7^\circ$ ^[13]) in the three 1C_4 forms in which the CH_2OH groups are directed towards the outside of the macrocycle versus a *gauche*-*gauche* arrangement ($\omega = -66.8^\circ$ ^[13]) in the three 4C_1 forms in which their equatorially disposed CH_2OH groups point towards the center of the macrocycle, thereby closing it (Figure 2). Accordingly, the disk-shaped molecule has a shallow

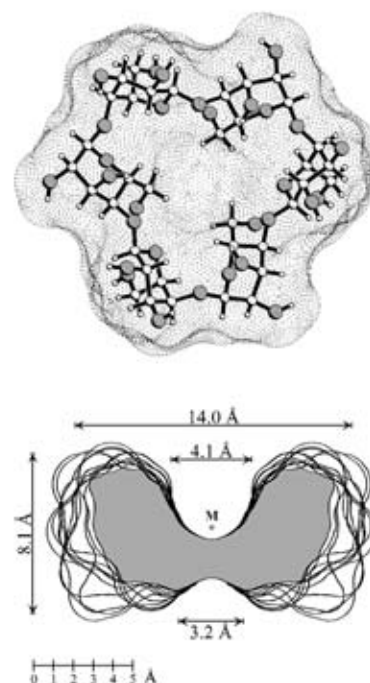


Figure 2. Top: Calculated [12] contact surface (in dotted form) of the solid-state structure of **1** with inserted ball-and-stick-model. The three equatorial hydroxymethyl groups of the 4C_1 altropyranoses are directed towards the macrocycle's interior, thereby closing it. Bottom: Cross-sections through the contact surface of **1** (2-OH/3-OH side up) and approximate molecular dimensions: surface contours were obtained for a plane perpendicular to the macrocycle's mean plane through successive 10° rotation steps around the geometrical center M and subsequently superimposed.

indentation on one side, and a pronounced hole-like depression on the other. Provided that this disk-shaped, solid-state structure of **1**, already embedded in a water matrix, is retained in aqueous solution, not only separate sets of NMR signals should be observed for the 4C_1 and the 1C_4 portions, but also distinctly different coupling patterns for the respective pyranoid ring protons as revealed by the calculated J values (Table 1).

The high resolution 1H and ${}^{13}C$ NMR spectra of **1** in D_2O ,^[14] however, unambiguously provide only one set of signals for both the altropyranoid hydrogen atoms and the carbon atoms, and the 1H coupling constants are an average of those calculated for the 4C_1 and 1C_4 conformations (Table 1); moreover, the observed J -values correlate surprisingly well with those calculated for the all-skew (twist-boat) 0S_2 geometry of **1c**, which, in

Table 1. Dihedral angles as well as the ^1H – ^1H coupling constants measured in D_2O (800 MHz [14], 30 °C) and those calculated for the altropyranoid ring in $^4\text{C}_1$, $^1\text{C}_4$, and all- $^0\text{S}_2$ (skew) forms of **1**.

	$^4\text{C}_1$ [a]	$^1\text{C}_4$ [a]	$^0\text{S}_2$ [b]	found
Dihedral angle [°]				
H1-C1-C2-H3	–69.4	–178.0	–138.3	
H2-C2-C3-H3	70.4	–176.0	–176.2	
H3-C3-C4-H4	–61.5	51.8	–44.7	
H4-C4-C5-H5	–71.3	179.8	–141.9	
Coupling constant [Hz] [c]				
$J(1,2)$	2.2	8.0	4.0	4.73
$J(2,3)$	2.7	10.2	10.2	8.19
$J(3,4)$	3.4	2.4	4.5	3.71
$J(4,5)$	9.7	1.4	6.4	5.32

[a] Angles from the solid-state structure of **1**. [b] Data calculated for the global energy minimum (all-skew form) from HTA simulations. [c] Calculation based on the Karplus-type dependence of H-C-C-H torsion angles on coupling constants, including the electronegativity effect of the substitution pattern by use of the generalized Haasnoot equation [15].

fact, emerges from extensive HTA calculations^[16] as the global energy minimum structure. Favored over the $^4\text{C}_1$ / $^1\text{C}_4$ solid-state geometry by as much as 36 kJ mol^{-1} —a major portion of this energy gain undoubtedly stems from hydrogen bonding between the 2-OH of one altrose moiety to the O-3 of the next—this all-skew form features a cavity that pierces the disk (Figure 3) and a pyranose tilt inverse to that of the cyclodextrins.

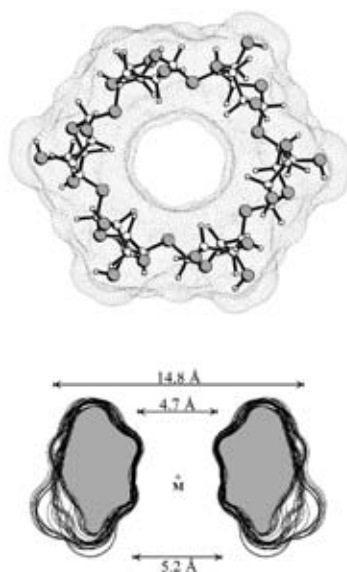


Figure 3. The all-skew (twist-boat) $^0\text{S}_2$ -geometry of α -cycloaltrin (**1**) emerging from HTA simulations [16] as the global energy minimum structure. Top: Contact surface. Bottom: The contour plots reveal a cavity whose conicity is inverse to that of the cyclodextrins.

Whether, however, the all-skew form **1e** is adopted in aqueous solution—in HTA simulations molecules are in vacuum rather than surrounded by a solvation shell—remains open. If prevalent in aqueous solution, its cavity is conceivably filled with water. Thus not only the six primary, but also the 12 secondary hydroxyl groups are likely to satisfy their hydrogen bonding requirements towards the solvent rather than intramolecularly. This results in a tightly associated first water shell around **1**, which will have to follow any geometry changes within the macrocycle. This hydration sphere could readily be character-

ized by molecular dynamics (MD) simulations in water, but contributed little to unraveling the nature of the $^4\text{C}_1 \rightleftharpoons ^1\text{C}_4$ scrambling observed in the NMR spectra, since on subjection to a 600 ps MD simulation in a box of water,^[17] not only the geometry of the hydrated all-skew $^0\text{S}_2$ form (**1c**), but also that of the solid-state $^4\text{C}_1$ / $^1\text{C}_4$ structure **1d**, remained in their respective geometries (Figure 4). Accordingly, no appreciable flexing

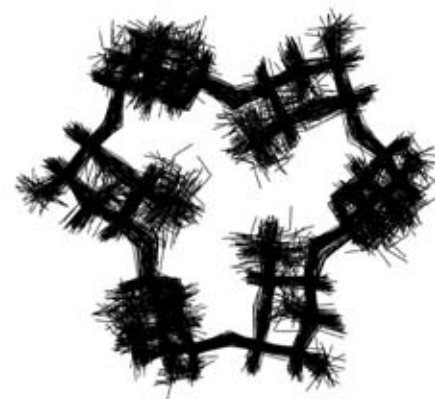


Figure 4. Superimposition of 60 α -cycloaltrin snapshot-geometries taken in 10 ps intervals from a 600 ps molecular dynamic simulation [17] on an assembly comprising α -cycloaltrin in a box of 606 water molecules.

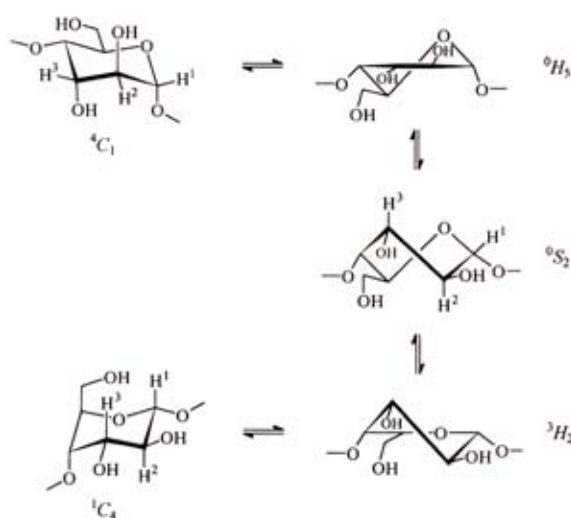
or flip over of the pyranoid chairs or skew forms to alternate topologies takes place within a 600 ps time frame; that is, profound conformational changes like the flipping from $^4\text{C}_1$ to $^1\text{C}_4$ within the macrocycle are comparatively slow, and require the 10^6 times longer, millisecond time frame of NMR spectroscopy to become observable.

The temperature-dependent ^1H and ^{13}C NMR studies proved to be more meaningful in determining the nature of the conformational changes occurring in aqueous solutions of **1**:^[14] the coupling constant $J_{2,3}$ of 8.2 Hz at 30 °C in D_2O decreases to 7.6 and 7.1 Hz at 20 and 4 °C, respectively, thereby narrowing the well-separated signal for 3-H; more profound effects are observed for the C-4 and C-5 signals, which, like all other carbon atoms, give rise to sharp singlets at 30 °C but show substantial broadening at 4 °C, which indicates the onset of “freezing out” certain conformations the $^4\text{C}_1 \rightleftharpoons ^1\text{C}_4$ equilibrium. Consequently, in water, α -cycloaltrin does not adopt a fixed geometry, such as the all- $^0\text{S}_2$ -form; rather, the D-altropyranoid rings, tied up in a macrocyclic “straitjacket”, adopt a variety of conformations within the $^4\text{C}_1 \rightleftharpoons ^0\text{S}_2 \rightleftharpoons ^1\text{C}_4$ pseudorotational “turntable” (Scheme 3), and this necessarily in a coordinated way: flexure of one altropyranoid chair into the intermediate skew $^0\text{S}_2$ -form via half-chair transition states forces the two adjoining altrose chairs to follow suit, thereby eliciting a consecutive “rolling around” in the probably elliptically distorted macrocycle. NMR data provide an averaged picture thereof and give evidence through the comparatively large $J_{1,2}$ and, particularly, $J_{2,3}$ couplings that the position of the equilibrium in water at 30 °C lies pronouncedly on the $^1\text{C}_4 \rightleftharpoons ^0\text{S}_2$ side.

Experimental Section

3: To a solution of NaH (0.40 g, 10.8 mmol) in anhydrous DMF (40 mL) was added **2** (1.0 g, 0.6 mmol) [9], and the mixture was kept under N_2 at 60 °C for 2 h. After cooling, benzenesulfonyl chloride (568 μL , 4.32 mmol) in anhydrous DMF (10 mL) was injected followed by stirring at room temperature for 30 min. Filtration and flash chromatography on a silica gel column (4 \times 15 cm) with benzene/EtOAc (4/1, 250 mL) afforded 600 mg (64%) of **3**; m.p. 203 °C (decomp.); $[\alpha]_D^{20} = +70.1$ ($c = 0.36$ in THF). ^1H NMR (500 MHz, CDCl_3 , relevant data): $\delta = 3.11$ (d, 1H, 2-H), 3.32 (d, 1H, 3-H), 3.56 and 4.24 (two d, 1H, 6-H₂), 3.64 (d, 1H, 4-H), 3.93

COMMUNICATIONS



Scheme 3. The chair/half-chair/skew pseudorotational "turntable" between α -tropanoid rings in 4C_1 and 1C_4 conformation [18]. Due to the comparatively large $J_{1,2}$ and $J_{2,3}$ values found for **1** (4.7 and 8.2 Hz, respectively, in D_2O), the conformational equilibrium in aqueous solution lies on the ${}^1C_4 \rightleftharpoons {}^3H_2 \rightleftharpoons {}^0S_2$ side.

(m, 1H, 5-H), 5.16 (s, 1H, 1-H), $J_{1,2}$ and $J_{2,4} = 0$, $J_{2,3} = 3.7$, $J_{4,5} = 11.5$ Hz. MS: $[M^+]$ not detectable. Elemental analysis calculated for $C_{72}H_{132}O_{24}Si_6$: C 55.78, H 8.58; found: C 55.55, H 8.68.

4: A 1 M solution of Bu_4NF in THF (4.6 mL) was added to a solution of silyl epoxide **3** (1.0 g, 0.65 mmol) in anhydrous THF (90 mL) under N_2 , and the mixture was stirred at 40 °C for 4 h. Concentration in vacuo, addition of methanol (10 mL), and cooling in a refrigerator overnight resulted in a precipitate: 511 mg (92%) of **4**; m.p. 166 °C (decomp.); $[\alpha]_D^{25} = +83.6$ ($c = 0.34$ in DMSO). 1H NMR (500 MHz, D_2O , pyridine): $\delta = 3.40$ (d, 1H, 2-H), 3.67 (d, 1H, 3-H), 4.10 (m, 1H, 5-H), 4.30 (m, 2H, 6-H₂), 4.47 (d, 1H, 4-H), 5.57 (s, 1H, 1-H), $J(1,2)$ and $J(3,4) = 0$, $J(2,3) = 3.5$, $J(4,5) = 11.6$ Hz; FAB-MS: m/z : 865 $[M^+]$.

1: A solution of epoxide **4** (1.0 g, 1.14 mmol) in distilled water (250 mL) was heated at reflux for 5 days. Concentration of the mixture in vacuo and chromatography on a reversed-phase column (Merck Lobar, size C) with water yielded **1** (765 mg (68%); m.p. 215 °C (decomp.); $[\alpha]_D^{25} = +70.5$ ($c = 0.3$ in H_2O)). 1H NMR (800 MHz [14], D_2O , 30 °C): $\delta = 3.91$ (dd, 1H, 6-H₂), 4.00 (m, 2H, 2-H, 6-H₂), 4.03 (dd, 1H, 3-H), 4.14 (dd, 1H, 4-H), 4.44 (sext, 1H, 5-H), 4.95 (d, 1H, 1-H), $J_{1,2} = 4.73$, $J_{2,3} = 8.19$, $J_{3,4} = 3.71$, $J_{4,5} = 5.32$, $J_{5,6a} = 3.60$, $J_{5,6b} = 3.46$, $J_{6,a} = 12.42$ Hz. ${}^{13}C$ NMR (200 MHz [14], D_2O , 30 °C): $\delta = 63.05$ (C-6), 71.98 (C-3), 73.26 (C-2), 76.07 (C-5), 79.65 (C-4), 105.53 (C-1). FAB-MS: m/z : = 973 $[M + H^+]$, 995 $[M + Na^+]$.

Received: February 19, 1997 [Z101391E]

German version: *Angew. Chem.* **1997**, *109*, 1987–1991

Keywords: α -cyclomaltrin • cyclodextrins • macrocycles • molecular modeling

- [1] a) J. Szejtli, *Cyclodextrins and Their Inclusion Complexes*, Akadémiai Kiadó, Budapest, **1982**; b) *Trends in Cyclodextrins and Derivatives*, (Ed.: D. Duchêne), Edition de la Santé, Paris, **1991**; c) G. Wenz, *Angew. Chem.* **1994**, *106*, 851–870; *Angew. Chem. Int. Ed. Engl.* **1994**, *33*, 803–822; d) *Proceedings of the 8th International Symposium on Cyclodextrins*, (Eds.: J. Szejtli, L. Szenté), Kluwer, Dordrecht, **1996**, p. 600 ff.
- [2] Recent review: F. W. Lichtenthaler, S. Immel, *J. Inclusion Phenom. Mol. Recognit. Chem.* **1996**, *25*, 3–16.
- [3] a) M. Kawamura, T. Uchiyama, T. Kuramoto, Y. Tamura, K. Mizutani, *Carbohydr. Res.* **1989**, *192*, 83–90; b) M. Sawada, T. Tanaka, Y. Takai, T. Hanafusa, T. Taniguchi, M. Kawamura, T. Uchiyama, *ibid.* **1991**, *217*, 7–17; c) The inulin-derived cyclodextrins, composed of six to eight $\beta(1 \rightarrow 2)$ -linked fructofuranose units, are disk-shaped molecules that are not pierced by the cavity [3d], and are hence unable to accommodate guests as the cyclodextrins can; due to their crown ether constitution, however, they exhibit cation binding properties [3b]; d) S. Immel, F. W. Lichtenthaler, *Liebigs Ann.* **1996**, 39–44.
- [4] M. Mori, Y. Ito, T. Ogawa, *Carbohydr. Res.* **1989**, *192*, 131–146; M. Mori, Y. Ito, J. Izawa, T. Ogawa, *Tetrahedron Lett.* **1990**, *31*, 3191–3194.
- [5] M. Nishizawa, H. Imagawa, Y. Kan, H. Yamada, *Tetrahedron Lett.* **1991**, *32*, 5551–5554; *Chem. Pharm. Bull.* **1994**, *42*, 1356–1365.
- [6] P. R. Ashton, C. L. Brown, S. Menzer, S. A. Nepogodiev, J. F. Stoddart, D. J. Williams, *Chem. Eur. J.* **1996**, *2*, 580–591.

- [7] F. W. Lichtenthaler, S. Immel, *Tetrahedron: Asymmetry* **1994**, *5*, 2045–2060.
- [8] a) S. J. Angyal, *Aust. J. Chem.* **1968**, *21*, 2737–2746; b) S. J. Angyal, V. A. Pickles, *ibid.* **1972**, *25*, 1695–1710.
- [9] K. Takeo, K. Uemura, H. Mitoh, *J. Carbohydr. Chem.* **1988**, *7*, 293–303.
- [10] K. Fujita, H. Shimada, K. Ohta, Y. Nogami, K. Nasu, T. Koga, *Angew. Chem.* **1995**, *107*, 1783–1784; *Angew. Chem. Int. Ed. Engl.* **1995**, *34*, 1621–1622.
- [11] Crystal structure analysis of **1**: $C_{36}H_{60}O_{30} \cdot 21 H_2O$, $M_r = 1351.18$, hexagonal, space group $P6_3$, $a = b = 17.241(3)$, $c = 13.323(2)$ Å, $V = 3430(1)$ Å³, $Z = 2$, $\rho = 1.268$ g cm⁻³, $\mu(MoK\alpha) = 0.115$ mm⁻¹, crystal dimensions $0.5 \times 0.15 \times 0.125$ mm, $T = 293$ K. Of 12711 reflections collected on a STOE IPDS diffractometer, graphite-monochromated $MoK\alpha$ ($\lambda = 0.71069$ Å) radiation, 2253 are independent ($R_{int} = 0.0284$). The structure was solved by direct methods (SHELXS-86) and successive Fourier difference synthesis. Refinement (on F^2) performed by full-matrix least squares method with SHELXL-93. $R(F) = 0.0568$ for 2036 reflections with $I \geq 2\sigma(I)$, $wR(F^2) = 0.1604$ for all 2253 reflections ($w = 1/(\sigma^2(F_o^2) + (0.1189 P)^2 + 0.57 P)$; $P = (F_o^2 + 2 F_c^2)/3$). All non-hydrogen atoms (except one oxygen atom of the solvent water molecule) were refined anisotropically. Hydrogen atoms on the cyclomaltrin were considered in calculated positions with the $1.2 U_{eq}$ value of the corresponding bound atom. Crystallographic data (excluding structure factors) for the structure reported in this paper have been deposited with the Cambridge Crystallographic Data Centre as supplementary publication no. CCDC-100196. Copies of the data can be obtained free of charge on application to The Director, CCDC, 12 Union Road, Cambridge CB2 1EZ, UK (fax: int. code + (1223) 336-0333; e-mail: deposit@chemcris.cam.ac.uk).
- [12] a) The color graphics (Figure 1) and the molecular contact surfaces (Figures 2 and 3) were generated with the MOLCAD molecular modeling program and its texture mapping option: J. Brickmann, *MOLCAD—MOLecular Computer Aided Design*, Technische Hochschule Darmstadt, **1992**. The major part of the MOLCAD program is included in the SYBYL package (TRIPOS Associates, St. Louis, USA); for details, see J. Brickmann, *J. Chim. Phys.* **1992**, *89*, 1709–1721; b) "Interactive Visualization of Molecular Scenarios with MOLCAD/SYBYL": J. Brickmann, T. Goetze, W. Heiden, G. Moeckel, S. Reiling, H. Vollhardt, C.-D. Zachmann, in *Insight and Innovation in Data Visualization* (Ed.: J. E. Bowie), Manning, Greenwich, **1994**, p. 83–97.
- [13] The orientation of the 6-OH groups relative to the pyranoid ring is defined by the exocyclic torsion angles $O_5-C_5-C_6-O_6$ (ω) and $C_4-C_5-C_6-O_6$; generally preferred are the *gg* and the *gr* forms where the first letter denotes the *gauche* orientation of O_6 towards the pyranoid ring oxygen and the other that of O_4 to C_4 .
- [14] The 1H (800 MHz) and ${}^{13}C$ (200 MHz) NMR spectra were recorded at the "Large Scale Facility for Biomolecular NMR" in Frankfurt. We are grateful to Prof. Dr. C. Griesinger and Dr. H. Schwalbe, Institut für Organische Chemie, Universität Frankfurt am Main, for support.
- [15] C. A. G. Haasnoot, F. A. A. M. De Leeuw, C. Altona, *Tetrahedron* **1980**, *36*, 2783–2792.
- [16] High-temperature annealing (HTA) calculations were performed with a force field program specially adapted to carbohydrates, comprising application of the verlet integrator in the MD simulation program CHARMM with a time step of 1 fs at constant temperature and dielectric constant $\epsilon = 1$. Every 1000 fs the respective conformation from the MD trajectories at 1200 K (4059 ps) was allowed to cool down to 300 K with a rate of 10 K fs⁻¹, was held there for an additional 1100 fs, and was subsequently fully energy-minimized by an adapted Newton–Raphson algorithm of the CHARMM22 program package with a convergence criterion of 10^{-7} kcal mol⁻¹. For **1**, a total of 2736 (67%) different conformers (corresponding to 16416 altrose units) underwent geometry analysis.
- [17] The CHARMM force field with **1** in the center of a truncated octahedron ($V \approx 16400$ Å³) was used for the MD simulations, and the remaining empty space was filled with water molecules.
- [18] For conformational notations see IUPAC–IUB Recommendations, *Pure Appl. Chem.* **1981**, *53*, 190–195; *Carbohydr. Res.* **1997**, *297*, 20–21.

Molecular Modeling of Saccharides, Part 21^[‡]Solution Geometries and Lipophilicity Patterns of α -Cycloaltrin**Stefan Immel, Kahee Fujita, and Frieder W. Lichtenthaler*^[a]

Abstract: Detailed analysis of the conformational features of α -cycloaltrin (**1**) in aqueous solution by temperature dependent ¹H and ¹³C NMR studies, together with molecular dynamics simulations, reveal that the six altropyranose units are in a complex dynamic equilibrium within the ⁴C₁ ⇌ ⁰S₂ ⇌ ¹C₄ pseudorotational turntable. This gives rise to a large number of macrocyclic conformations, ranging from a disk-shaped molecule with a hydrophobic

central hole (alternating ⁴C₁/¹C₄ form **1a**) to a torus form of the macrocycle with an equally hydrophobic through-going cavity (all skew-boat form **1b**). Constrained MD simulations throw light on the conformational transitions be-

tween these two extreme forms (**1a** ⇌ **1b**). Flexure of one altropyranoid chair into the skew-boat-⁰S₂ form forces adjoining altropyranoid units to follow suit, thereby eliciting a successive, synergistic “rolling around” within the, on average, elliptical macrocycle. Thus, α -cycloaltrin is the first thoroughly flexible cyclooligosaccharide and can be used to probe the induced-fit mode of guest–host interactions.

Keywords: α -cycloaltrin • cyclodextrins • lipophilicity patterns • molecular dynamics • molecular modeling • solution geometries

Introduction

Research towards cyclooligosaccharides made from sugar units other than glucose^[2–11] has been undertaken throughout the last decade. The foremost incentive in this pursuit is the generation of molecular receptors with recognition features different from those of the well-studied, overly rigid cyclodextrins (CDs). Unfortunately, only the inulin-derived^[3a] cyclofructins with six and seven $\beta(1 \rightarrow 2)$ -linked fructofuranose units became accessible in quantities sufficiently large to

demonstrate their ability to complex metal cations.^[12] The guest-complexation behavior of all other non-glucose cyclooligosaccharides could only be assessed by molecular modeling studies. Those composed of D-mannose (α - and β -cyclomannin^[4]) and L-rhamnose (α -cyclorhamnin^[5]), or both,^[9] have their axially oriented 2-OH group directed towards the outside of the macrocycle, as evident from the contact surface and cross section plot for α -cyclomannin (Figure 1). A somewhat smaller torus height than in α -cyclodextrin results, yet this has no principal effect on the backbone structure, the cavity dimensions, or the lipophilicity pattern.^[6, 10] A similar α -CD-like geometry was found for a cyclogalactin consisting of six $\beta(1 \rightarrow 4)$ -linked galactopyranose residues (Figure 1, top right), yet its lipophilicity profile is different because hydrophobic surface regions at the primary hydroxyl face are substantially enlarged.^[6]

More profound changes in shape, cavity dimensions, and guest-binding properties are to be anticipated for cyclooligosaccharides with axially disposed 3-OH groups in their pyranoid rings, since these 3-OH groups are directed towards the interior of the cavity. As illustrated in Figure 1 for the hexameric α -cycloallin, steric congestion resulting therefrom induces the altropyranose units to adopt a wide range of tilt angles relative to the macrocycle and a substantial narrowing of the 2-OH/3-OH side of the torus, yet the pyranoid ⁴C₁ geometries are retained without exception.^[14]


For cyclic oligosaccharides composed of D-altropyranoses—those with six (α -cycloaltrin **1**^[11]), seven,^[7] and eight $\alpha(1 \rightarrow 4)$ -linked units^[8] have recently become accessible from

[a] Prof. Dr. F. W. Lichtenthaler, Prof. K. Fujita,^[‡] Dr. S. Immel
Institut für Organische Chemie, Technische Universität Darmstadt
Petersenstrasse 22, D-64287 Darmstadt (Germany)
Fax: (+49) 6151-166674
E-mail: fwlicht@sugar.oc.chemie.tu-darmstadt.de

[+] Permanent address:
Faculty of Pharmaceutical Sciences, Nagasaki University
Nagasaki 852-8131 (Japan)

[‡] Presented in part at the XIXth International Carbohydrate Symposium, San Diego (USA), August 1998; Abstract A 124. Part 20: K. Fujita, W.-H. Chen, D.-Q. Yuan, Y. Nogami, T. Koga, T. Fujioka, K. Mihashi, S. Immel, F. W. Lichtenthaler, *Tetrahedron: Asymmetry* **1999**, *10*, 1689–1696.

[**] A cyclooligosaccharide composed of six $\alpha(1 \rightarrow 4)$ -linked D-altropyranose residues; for derivation of the terminology used see ref. [1]

 Supporting information for this article in the form of 3D structures of Figure 1 and MOLCAD graphics is available on the WWW under <http://caramel.oc.chemie.tu-darmstadt.de/imm1/3Dstructures.html> and <http://caramel.oc.chemie.tu-darmstadt.de/imm1/molcad/gallery.html>, respectively.

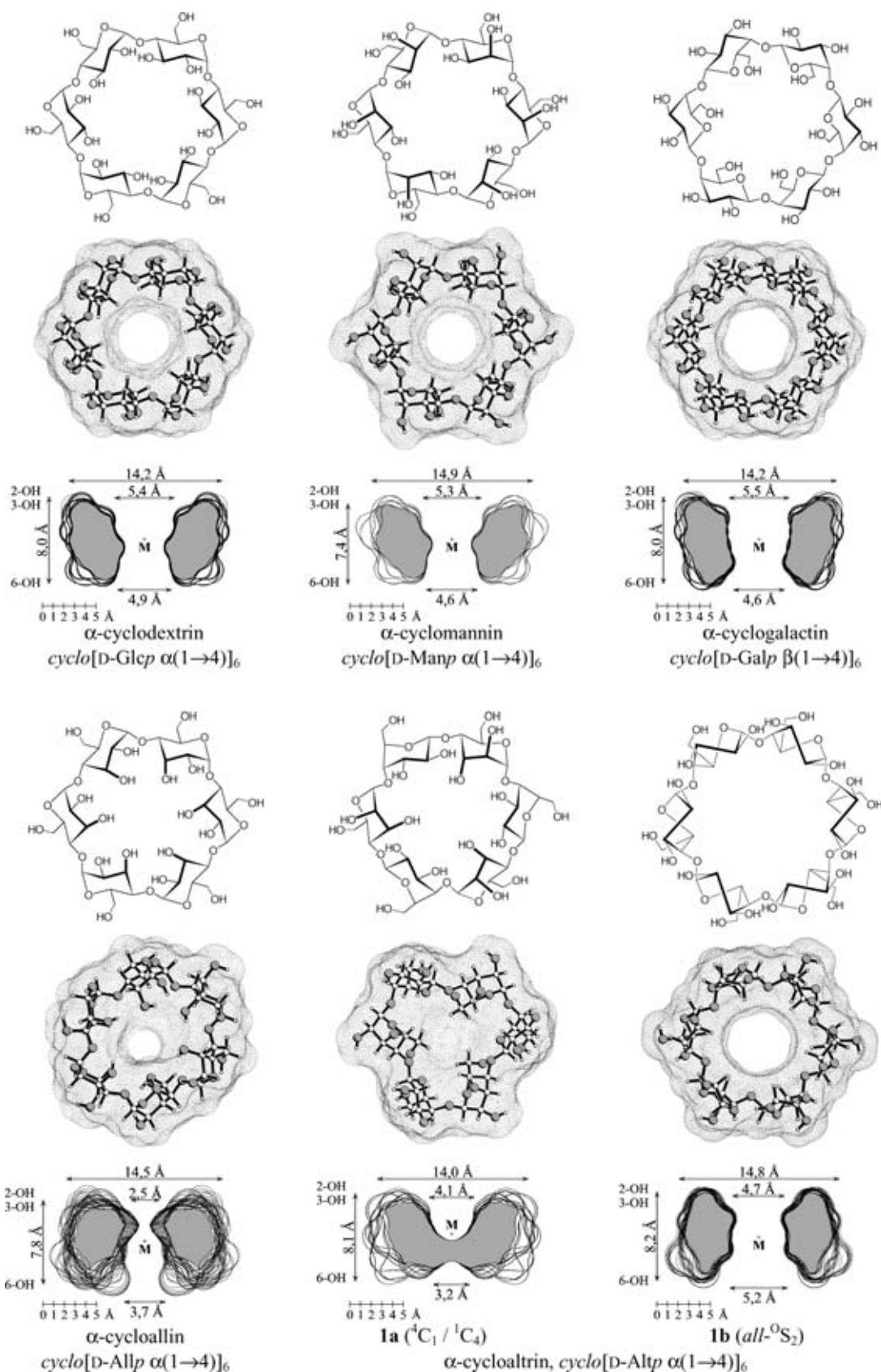


Figure 1. Molecular geometries of α -cyclodextrin^[13] compared to cyclooligosaccharide analogues composed of six identical hexopyranose residues in their macrocycle: D-mannose (α -cyclomannin^[6]), D-galactose (α -cyclogalactin^[6]), D-allose (α -cycloallin^[14]), and D-altrose (α -cycloaltrin, in its solid-state form **1a** and the *all-skew-O₂* geometry **1b** emerging from HTA simulations as the global minimum energy structure^[10, 11]). Conventional chemical formulas (top entries), calculated contact surfaces (in dotted form with ball-and-stick-model insert, center), and cross-section plots with approximate molecular dimensions (2-OH and 3-OH sides up) are depicted.

the respective cyclodextrins in a high-yielding four-step procedure—retention of the 4C_1 geometry for the altropyranoid rings (with axially disposed 2-OH and 3-OH groups) is highly unlikely, since there is ample calculatory^[15] and 1H NMR evidence^[16] that α -D-altropyranose itself and a variety of its simple derivatives establish a dynamic equilibrium within the ${}^4C_1 \rightleftharpoons {}^1C_4$ pseudorotational “turntable” (Figure 2). X-ray crystallography revealed that α -cycloaltrin

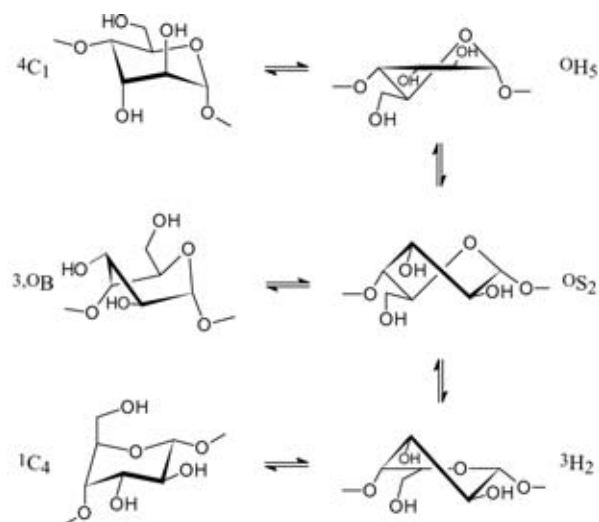


Figure 2. The chair/half-chair/skew (twist-boat) pseudorotational itinerary between α -D-altropyranoid rings in 4C_1 and 1C_4 conformation. The ${}^{3,0}B$ and ${}^{1,0}S_2$ forms are closely related to each other, hence have similar coupling constants and are not differentiated in Table 1 and Figure 4; the two half-chair conformations 3H_5 and 3H_2 appear to be higher in energy and are transition states in the ${}^4C_1 \rightleftharpoons {}^1C_4$ conformational itinerary.

adopts an architecturally unprecedented macrocyclic structure comprising an alternating sequence of 4C_1 and 1C_4 pyranoid chair conformations, resulting in a disk-shaped molecule with a central indentation rather than a through-going cavity (Figure 1, **1a**).^[11] This unique topography in the solid state, in spite of being embedded into a matrix of 21 water molecules, does not survive on dissolution in water, for only one set of 1H NMR signals are observed.^[11] This finding is compatible with either of the following two scenarios: operation of a dynamic equilibrium between the 4C_1 and 1C_4 chairs within the pseudorotational transitions illustrated in Figure 2, whereby NMR measurements average over the variety of macrocyclic conformations, or alternatively, adoption of a fixed conformation, an *all*-

skew (twist-boat) form conceivably, as this form emerges from high-temperature annealing (HTA) simulations as the global energy minimum structure (**1b** in Figure 1). Notably, this *all*- 0S_2 form **1b** contains a cavity that is larger and possesses the opposite concavity than that of α -cyclodextrin, and **1b** should therefore be able to form inclusion complexes with sterically matching guests.

A detailed study towards a differentiation between these possibilities appeared warranted since—should a dynamic equilibrium prevail in solution—the cycloaltrins would be the first thoroughly flexible cyclooligosaccharides capable of adapting their overall geometries to binding of appropriate guests, a process that more closely corresponds to Koshland’s induced-fit mode of substrate-receptor interaction^[17] than to the overly static lock-and-key model.^[18] These issues are herein explored by temperature-dependent NMR analysis, standard and constrained MD simulations, and generation of the lipophilicity patterns of the closed and open forms **1a** and **1b**.

Results and Discussion

Temperature-dependent NMR analysis: High-resolution 1H and ${}^{13}C$ NMR spectra of α -cycloaltrin (**1**) in D_2O (Figure 3) display only one set of signals for the six altropyranoses, indicating either fast averaging between different altropyranoid ring conformations, or alternatively adoption of a uniform geometry somewhere in between the 4C_1 and 1C_4 conformation for all six altrose units. Experimental 1H NMR coupling constants (Table 1) are consistent with either scenario.

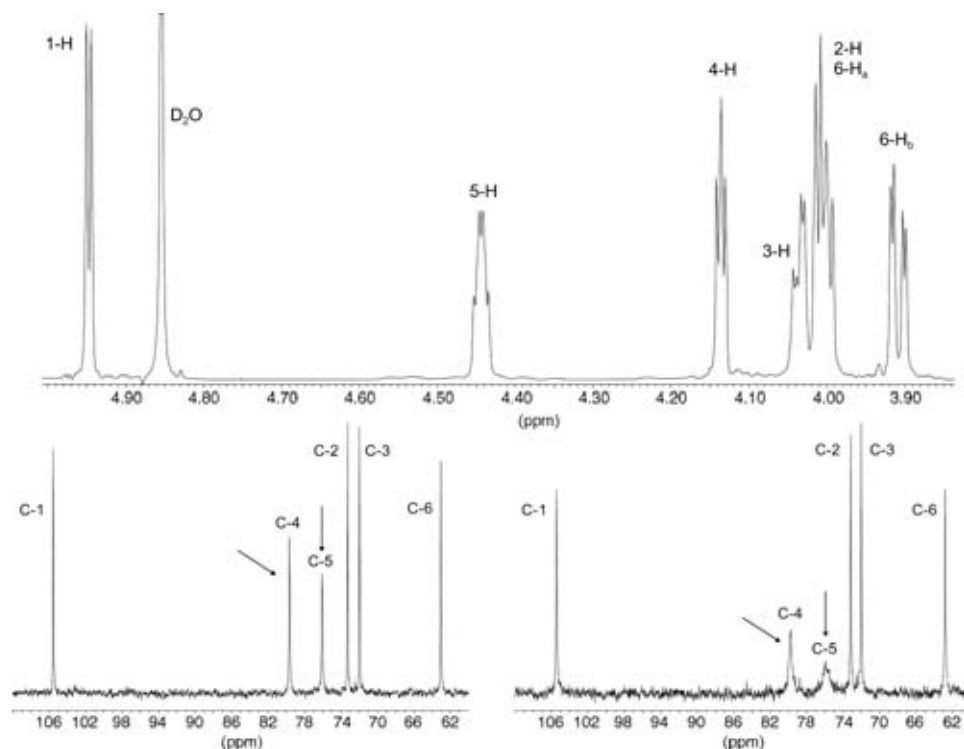


Figure 3. Top: 800 MHz 1H NMR spectrum of α -cycloaltrin (**1**) in D_2O at 30 °C reveals one set of signals. Bottom: 200 MHz ${}^{13}C$ NMR spectra of **1** in D_2O at 32 °C (left) and 4 °C (right). As indicated by the arrows, the signals of C-4 and C-5 are significantly broadened at lower temperatures.

FULL PAPER

F. W. Lichtenthaler et al.

Table 1. Comparison of the altopyranoid ring ^1H - ^1H -coupling constants for α -cycloaltrin (800 MHz, D_2O , 30°C) with those calculated for its $^4\text{C}_1$, $^1\text{C}_4$, and all- $^{\circ}\text{S}_2$ (skew) forms.

J_{HH} [Hz]	Found	Calculated ^[a] for			
		$^4\text{C}_1$ ^[b]	$^1\text{C}_4$ ^[b]	$^{\circ}\text{S}_2$ ^[c]	$^4\text{C}_1/{}^1\text{C}_4/{}^{\circ}\text{S}_2$ ^[d]
$J_{1,2}$	4.73	2.2	8.0	4.0	4.9
$J_{2,3}$	8.19	2.7	10.2	10.2	8.3
$J_{3,4}$	3.71	3.4	2.4	4.5	3.5
$J_{4,5}$	5.32	9.7	1.4	6.4	5.5

[a] Calculation based on the Karplus-type H-C-C-H torsion angle dependency of coupling constants, including the electronegativity effect to the substitution pattern by use of the generalized Haasnoot equation.^[19]

[b] Values obtained for the pyranose conformations realized in the crystal structure **1a**. [c] Data resulting from calculations on the HTA-derived global energy minimum all-skew form **1b**.^[10, 11] [d] Least-squares fit for 26% $^4\text{C}_1$, 34% $^1\text{C}_4$, and 40% $^{\circ}\text{S}_2$, roughly corresponding to a 1:1:1 mixture of conformers.

The presence of a dynamic conformational equilibrium in aqueous solution is inferred from the temperature dependence of the ^1H NMR data: the value for $J_{2,3}$ decreases from 8.2 Hz at 30°C to 7.6 and 7.1 Hz at 20 and 4°C , respectively, thereby narrowing the well-separated signal for H-3. Although the smaller value of $J_{2,3}$ at 4°C suggests a more intensely populated $^4\text{C}_1$ altrose conformation in the $^4\text{C}_1 \rightleftharpoons ^{\circ}\text{S}_2 \rightleftharpoons ^1\text{C}_4$ pseudorotational itinerary, the best fit of calculated^[19] versus measured coupling constants emerging from the

triangle representation of Figure 4, revealed a composition of 26% $^4\text{C}_1$, 34% $^1\text{C}_4$, and 40% $^{\circ}\text{S}_2$ (cf. center minimum of σ -contours at 0.18 Hz), indicating, within the margin of error, the presence of essentially equal proportions of the three forms.

More profound temperature effects are observed for the ^{13}C signals of C-4 and C-5, which are substantially broadened on lowering the temperature from 30 to 4°C (cf. Figure 3). This is clearly indicative of a dynamic equilibrium of various altopyranoid geometries which starts to “freeze out” at 4°C . However, the NMR data neither reveal which of the many macrocyclic conformations within the sterically limiting “straitjacket” of **1** are preferred, nor answer the question of how the conformational transitions $\mathbf{1a} \rightleftharpoons \mathbf{1b}$ occur.

Molecular dynamics simulations: MD simulations with explicit incorporation of the (aqueous) solvent were performed for both α -cycloaltrin forms, **1a** and **1b**. Despite considerable flexibility in the macrocycles, no significant conformational transitions for the pyranose units were observed within a time frame of 600 ps (Figure 5). The solute hydration shells can be readily characterized from these calculations. An average of 30.6 ± 2.7 and 39.6 ± 3.4 water molecules are hydrogen-bonded to **1a** and **1b**, respectively. Any change of the altopyranose conformations entails substantial rearrangements in this tightly bound first hydration shell, rendering these processes too slow to be observable during standard MD simulations. The crucial role of water in the rearrangement process becomes particularly evident when comparing the MDs in solution with HTA simulations on α -cycloaltrin in vacuum: at high (1200 K) as well as at low temperatures (300 K) frequent and unhindered conformational transitions are observed for the altrose units in the isolated macrocycle.

The effects on the macrocycle of changing a $^4\text{C}_1$ altrose unit in the $^4\text{C}_1/{}^1\text{C}_4$ form **1a** along the $^4\text{C}_1 \rightarrow ^{\circ}\text{S}_2 \rightarrow ^1\text{C}_4$ pathway can be monitored within a reasonable nanosecond time frame by means of constrained MD techniques: two pyranose ring torsion angles $\text{O}_5\text{-C}_1\text{-C}_2\text{-C}_3$ and $\text{C}_3\text{-C}_4\text{-C}_5\text{-O}_5$ of one altrose unit are restrained in such a way that the $^4\text{C}_1$ conformation is forced to vary in the desired direction (Figure 6, gray shaded altrose residue **B**). As this ring flip is artificially induced, the neighboring unconstrained monosaccharide units—each in the $^1\text{C}_4$ form—are subject to considera-

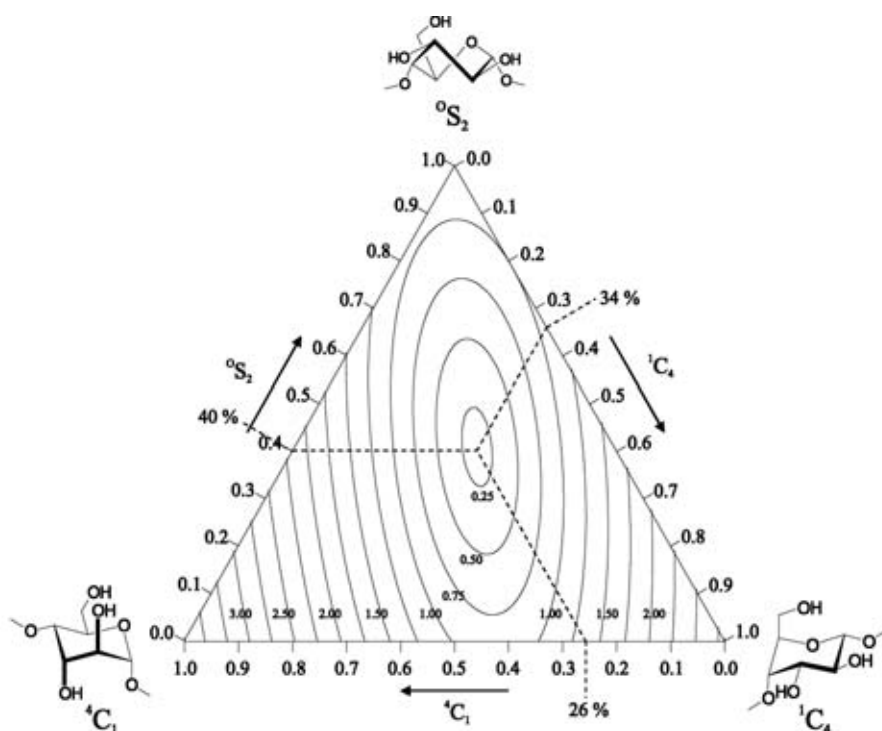


Figure 4. Triangular contour plot of the root-mean-square deviation (i.e. the error σ) of the calculated pyranose ring coupling constants ($J_{1,2}$, $J_{2,3}$, $J_{3,4}$, and $J_{4,5}$) versus those found experimentally. Contours are given as a function of the altrose conformational equilibrium between $^4\text{C}_1$ (left corner of the triangle), $^1\text{C}_4$ (right), and $^{\circ}\text{S}_2$ forms (top corner), and are plotted at levels of $\sigma = 0.25$ to 4.00 Hz in 0.25 Hz steps; the triangle axes are in units of molecular fractions $\chi_i = 0.0$ –1.0. The $^3J_{\text{HH}}$ coupling constants for the pure $^4\text{C}_1$, $^1\text{C}_4$, and $^{\circ}\text{S}_2$ pyranose forms (triangle corners) were obtained from the solid-state structure and the minimum-energy geometry of **1**. The values are listed in Table 1. The best-fit of calculated versus experimental data (center minimum of the σ -contours at $\sigma_{\text{min}} = 0.18$ Hz) emerged for 26% $^4\text{C}_1$, 34% $^1\text{C}_4$, and 40% $^{\circ}\text{S}_2$ (equilibrium composition marked by hatched lines); all other mixtures yielded larger errors.

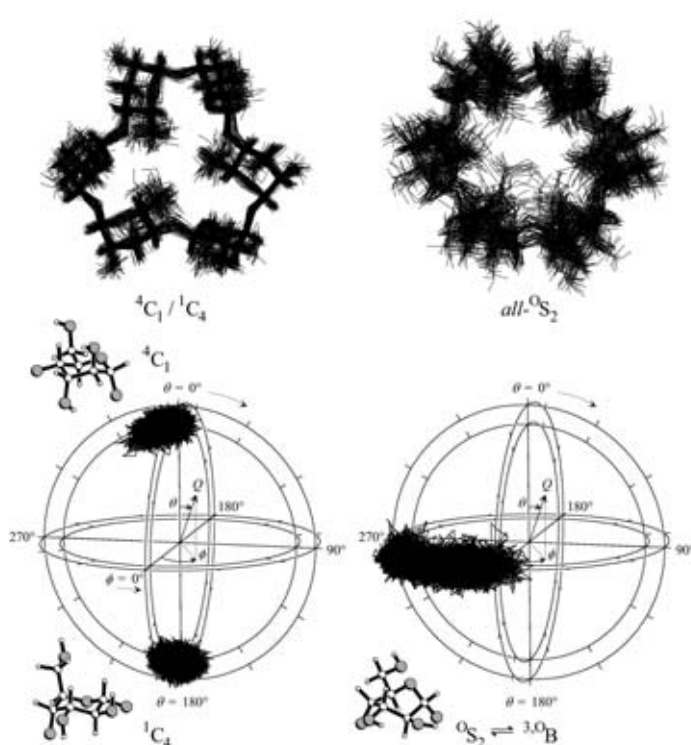


Figure 5. Top: Superimpositions of 60 α -cycloaltrin snapshot geometries taken in 10 ps intervals from MD simulations of **1a** (left) and **1b** (right) in water illustrate the flexibility of the macrocycles, despite relative conformational rigidity of the pyranose rings. Bottom: Polar-coordinate plots of the pyranose Cremer–Pople ring-puckering parameters^[28] derived from MD simulations of **1a** (left plot, solid-state structure) and **1b** (right, HTA-derived start geometry) in water. In both cases a time series (trajectory) of the pyranose pucker parameters Q , ϕ and θ is plotted in 3D-polar coordinates (height, longitude, and latitude): On the left, the well-separated trajectories for the 4C_1 and 1C_4 altrose units lack any conformational transitions between the different chair geometries within the MD time frame of approximately 600 ps; similarly, **1b** displays no significant deviations from the ${}^0S_2 \rightleftharpoons {}^3,0B$ geometries during the entire MD simulation.

ble intrinsic strain in the macro-ring: one is only slightly distorted towards the half-chair form (${}^1C_4 \rightarrow {}^3H_2$, unit **A** in Figure 6), whereas the residue on the other side (**C**) displays a full transition along ${}^1C_4 \rightarrow {}^0S_2 \rightleftharpoons {}^3,0B$. As this ring-flip was not induced by additionally applied MD potentials, it reveals the way conformational changes occur within the macrocycle: flexure of one altropyranoid chair into the intermediate skew- 0S_2 form via half-chair transition states forces the two adjoining altrose chairs, tied up in a macrocyclic “straitjacket” type clamp, to follow suit, and so on, thereby eliciting a consecutive “rolling around” in the probably elliptically distorted macrocycle.

As the above mechanism for interconversion involves energy concentration on one altrose unit (the restrained residue) with consecutive geometry changes in the macrocycle, there might be an alternative transition pathway: structural changes through excitation of low-energy macromolecular vibrational modes by thermal collisions with the solvent. Although such a mode of interconversion is difficult to induce through constrained MDs and was not observed during the standard MD simulations, it cannot be ruled out

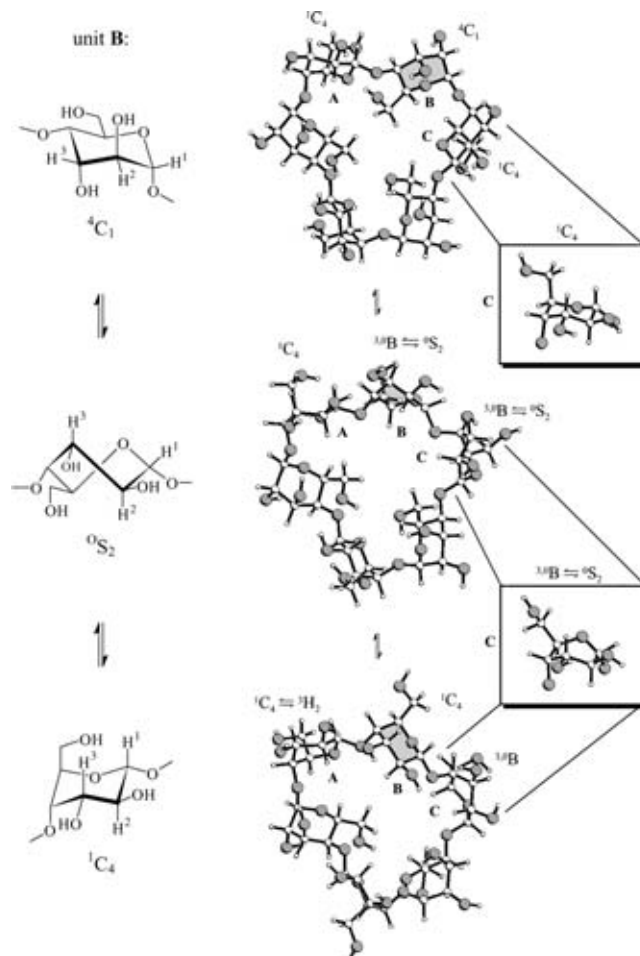


Figure 6. Constrained MD simulations of α -cycloaltrin exhibit a conformational transition of the central 4C_1 altropyranose (gray-shaded unit **B**) of a 1C_4 - 4C_1 - 1C_4 -fragment (units **A**-**B**-**C**) in the macrocycle: as **B** is driven along the ${}^4C_1 \rightarrow {}^3,0B/{}^0S_2 \rightarrow {}^1C_4$ reaction coordinate (formulas, left column), the conformation of the neighboring residue **A** varies very little with slight distortions ${}^1C_4 \rightarrow {}^3H_2$ only, but the altrose unit **C** cooperatively flips into a ${}^3,0B \rightleftharpoons {}^0S_2$ geometry (zoomed structures on the right). The unperturbed and cooperative conformational transitions of adjacent pyranose units point towards complex dynamic processes, in the course of which altrose residues cannot be considered independent; each conformational change induces new strains in neighboring units (all α -cycloaltrin snapshot structures were taken from a 130 ps MD perturbation, and constraints were applied to unit **B** only).

entirely. However, the question of whether structural changes in the macrocycle induce transitions in the monomers or vice-versa is bound to remain open as both conformational motions seem to be so intricately interwoven to the extent of being inseparable.

In either case, the overall result is a statistical scrambling over the 4C_1 , 0S_2 , and 1C_4 forms for the six altropyranose residues, of which the NMR data (Figure 3 and Table 1) provide an averaged picture. Although the distinct forms **1a** and **1b** cannot be identified directly from the NMR data presented in Figures 3 and 4, they should be taken into account as limiting structures in this complex conformational equilibrium.

Molecular lipophilicity patterns: Generation of molecular lipophilicity patterns (MLP)^[20] of the solid-state conformation

FULL PAPER

F. W. Lichtenthaler et al.

1a^[11] and of the HTA-derived energy-minimum *all*-⁰S₂ form **1b**^[10, 11] was achieved by the MOLCAD program,^[21] and was projected^[22] in color-coded form onto their contact surfaces^[23] depicted in Figure 1. The results displayed in Figure 7 allow a first assessment of the inclusion-complexation capabilities of α -cycloaltrin. Both the disk- (**1a**) and torus-shaped form (**1b**) reveal a distinct front–rear differentiation of hydrophobic and hydrophilic surface regions. The 2-OH, 3-OH side—in analogy to the cyclodextrins^[6, 10]—turns out to be the most hydrophilic part of the molecule, in contrast to a significantly more hydrophobic reverse side owing to the primary 6-CH₂OH groups. Although **1a** lacks a central “through-going” cavity, this conformer has a hydrophilic surface indentation and an outer core made up of irregularly distributed hydrophilic and hydrophobic regions (Figure 7,

top right). In contrast, the cyclodextrin-like, torus-shaped form **1b** displays a more uniform pattern of the corresponding surface qualities (Figure 7, bottom): the most hydrophobic surface areas extend from the 6-CH₂OH side well into the cavity, yet the tilt of the pyranose units in the macrocycle is the inverse of that present in α -cyclodextrin (Figure 1, top left).

Conclusion

These results provide unambiguous insight into the solution geometries of α -cycloaltrin (**1**) and into the comparable stabilities of the ⁴C₁- and ¹C₄-chair forms of its altropyranose residues. A large variety of macrocyclic shapes are possible within the constraints of its cyclohexasaccharide “straitjack-

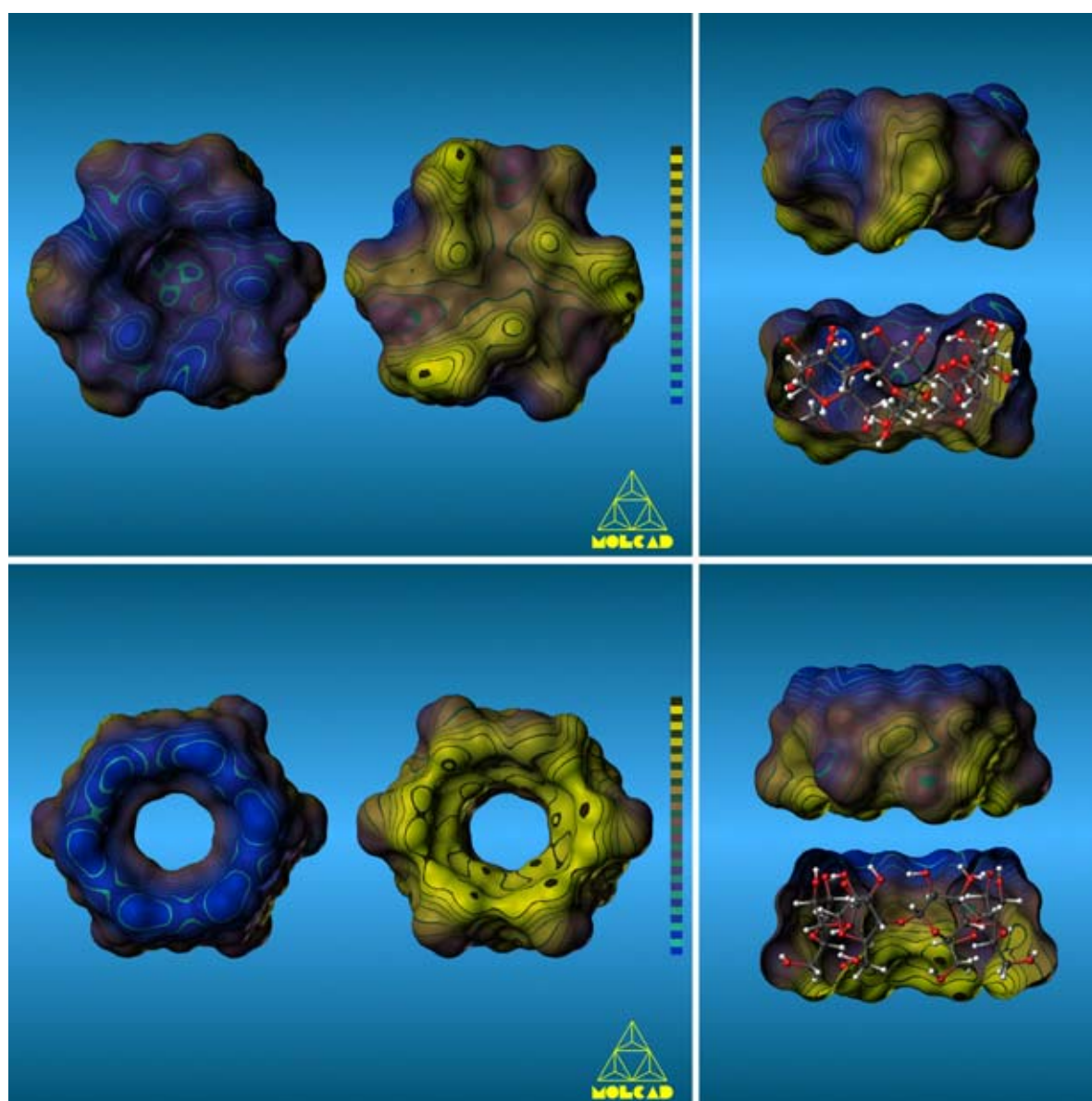


Figure 7. Molecular lipophilicity patterns of α -cycloaltrin (**1**) projected onto the contact surfaces of the solid-state conformation (**1a**, top) and the *all*-⁰S₂ form (**1b**, bottom). The color code applied ranges from dark blue for the most hydrophilic surface areas to full yellow corresponding to the most hydrophobic regions. On the left, the macrocycles are viewed from both sides perpendicular to the mean ring plane, exposing either the pronouncedly hydrophilic (blue) 2-OH/3-OH side of the torus or the opposite, hydrophobic rim made up from the primary 6-CH₂OH hydroxyl groups. The graphics on the right display the corresponding side views in closed and bisected form each, with the 2-OH and 3-OH groups directed upwards and the CH₂OH moieties at the lower rim.

et”. The shapes range from a disk-shaped macrocycle with a distinctly hydrophobic central hole, which is realized when the pyranose units adopt an alternating sequence of 4C_1 and 1C_4 conformations (**1a**), to a torus shape with an equally hydrophobic through-going cavity, realized when all pyranoid rings are in the skew-boat- 0S_2 form (**1b**). Both forms are limiting structures of a complex dynamic equilibrium. Accordingly, α -cycloaltrin (**1**) constitutes the first thoroughly flexible cycloligosaccharide with which to realistically probe the induced-fit mode^[17] of guest–host interactions. All previous utilizations of the overly rigid cyclodextrins as artificial enzymes^[24] have only served as models for the stationary lock-and-key type^[18] of enzyme action.

First evidence from capillary electrophoresis studies indicates that α -cycloaltrin and 4-*tert*-butylbenzoate form inclusion complexes. We hope that a sufficiently large number of guests interacting with α -cycloaltrin will justify broad exploration of this system.

Experimental Section

Temperature-dependent 1H (800 MHz) and ${}^{13}C$ (200 MHz) spectra were recorded at the “Large Scale Facility for Biomolecular NMR” of the University of Frankfurt.

HTA^[10, 11] and MD calculations were carried out using the CHARMM^[25] force field for carbohydrates^[26] and application of periodic boundaries (MDs, truncated octahedron filled with 606 (**1a**) and 611 (**1b**) water molecules, box size approximately 32 Å), isothermal ($T=300$ K), and isobaric conditions ($p=1$ bar) during a simulation time of 600 ps (equilibration time 25 ps, time step 1 fs); analysis of the MD trajectories was accomplished with external computer programs.^[27]

Constrained MD computations of α -cycloaltrin (cf. Figure 6) were carried out using the isothermal and isobaric simulation system as described above. Starting from the solid-state conformation **1a**, the ring torsion angles $O_5-C_1-C_2-C_3$ (θ_1) and $C_3-C_4-C_5-O_5$ (θ_4) of one altropyranose unit were constrained and driven during 39 independent MD runs with steps of 3° each, forcing one 4C_1 altrose geometry to vary slowly into the inverted 1C_4 conformation (“reaction parameters” θ_1 : $+57^\circ \rightarrow -57^\circ$, θ_4 : $-57^\circ \rightarrow +57^\circ$). Each MD trajectory was carried out for a 10 ps equilibration and a 25 ps data acquisition period, the final structures were used as a starting point for the next MD run after re-setting the torsion angles to the new values along the reaction coordinate. The conformational transitions of the remaining five unconstrained altrose residues were monitored by use of Cremer–Pople parameters.^[28]

Calculation of the molecular contact surfaces and the respective hydrophobicity potential profiles^[29] was performed by using the MOLCAD^[21] molecular modeling program and its texture mapping option.^[22] The MLP profiles were scaled in relative terms (most hydrophilic to most hydrophobic surface regions) for each molecule separately; no absolute values are displayed.

The minimum-energy structure of α -cycloaltrin was derived from a 675 ps MD study in water (CHARMM force field,^[25, 26] $T=300$ K, $p=1$ bar, 609 water molecules, parameters as above), with subsequent full energy minimization of a total of 13248 isolated solute structures by application of the PIMM91 force field,^[29] which is particularly suitable for carbohydrate structures without solvent.

Least-squares fitting of the J values for three conformations 4C_1 , 1C_4 , and 0S_2 was achieved with root-mean-square deviations of $\sigma_J=0.18$ Hz, whereas a two-state model ${}^4C_1 \rightleftharpoons {}^1C_4$ yielded $\sigma_J=0.80$ Hz.

Acknowledgements

We are grateful for financial support from Fonds der Chemischen Industrie, Frankfurt, and for a fellowship (to K.F.) from the Deutscher Akademischer Austauschdienst, Bonn. In addition, we thank Prof. Dr. C. Griesinger and Dr. H. Schwalbe, Goethe Universität Frankfurt, for recording the 1H

(800 MHz) and ${}^{13}C$ (200 MHz) NMR spectra, and Prof. Dr. J. Brickmann, Institut für Physikalische Chemie, Technische Universität Darmstadt, for providing access to his MOLCAD software package.

- [1] a) The naming of non-glucose cycloligosaccharides, in particular of those composed of different sugar units, can be exasperating. According to recent IUPAC Recommendations (*Carbohydr. Res.* **1997**, 297, 78 ff.), the systematic name for **1** turns out to be *cyclohexakis-(1 → 4)- α -D-altropyranosyl*, implying that **1** represents an assembly of “glycosyls” rather than being a “glycoside”. In fact it is a hexasaccharide. Alternatively the semi-systematic name *cyclo- α -(1 → 4)-D-altro-hexaoside*, abbreviated as “*cyclo[D-AltP α -(1 → 4)]₆”, may be used, based on a recent proposal for a simplified nomenclature,^[1b, 6] which has been authoritatively endorsed.^[1c] The most simple and practical designation, however—at least for cycloligosaccharides with a single type of sugar unit—is inferred from traditional CD terminology (dextrose being an old name for glucose), syllogistically leading to “cycloaltrin” and the Greek letters α , β , and γ designating the respective species with six, seven, and eight hexose units. Accordingly, **1** is appropriately termed *α -cycloaltrin*,^[11] and the next higher homologues, β -^[7] and γ -*cycloaltrin*.^[8] Correspondingly, other known non-glucose cycloligosaccharides with one type of monosaccharide unit are reasonably named α -, β -, and γ -*cyclomannin*,^[4, 6] *α -cyclohamnin*,^[5] and α - and β -*cyclofructin*.^[3] b) S. Immel, J. Brickmann, F. W. Lichtenthaler, *Liebigs Ann. Chem.* **1995**, 929–942; c) J. Szejtli, in *Comprehensive Supramolecular Chemistry, Vol. 3 (Cyclodextrins)*, (Eds.: J. Szejtli, T. Osa), Pergamon, Oxford, UK, **1996**, pp. 7 ff.; J. Szejtli, *Chem. Rev.* **1998**, 98, 1743–1753.*
- [2] L. V. Backinowsky, S. A. Nepogodiev, N. K. Kochetkov, *Carbohydr. Res.* **1989**, 185, C1–C3; L. V. Backinowsky, S. A. Nepogodiev, N. K. Kochetkov, *Tetrahedron* **1990**, 46, 139–150.
- [3] a) M. Kawamura, T. Uchiyama, T. Kuramoto, Y. Tamura, K. Mizutani, *Carbohydr. Res.* **1989**, 192, 83–90; b) M. Sawada, T. Tanaka, Y. Takai, T. Hanafusa, T. Taniguchi, M. Kawamura, T. Uchiyama, *Carbohydr. Res.* **1991**, 217, 7–17; c) S. Immel, F. W. Lichtenthaler, *Liebigs Ann. Chem.* **1996**, 39–44; d) S. Immel, G. E. Schmitt, F. W. Lichtenthaler, *Carbohydr. Res.* **1998**, 313, 91–105.
- [4] M. Mori, Y. Ito, T. Ogawa, *Carbohydr. Res.* **1989**, 192, 131–146; M. Mori, Y. Ito, J. Uzawa, T. Ogawa, *Tetrahedron Lett.* **1990**, 31, 3191–3194.
- [5] a) M. Nishizawa, H. Imagawa, Y. Kan, H. Yamada, *Tetrahedron Lett.* **1991**, 32, 5551–5554; *Synlett* **1992**, 447–448; b) M. Nishizawa, H. Imagawa, E. Morikuni, S. Hatekayama, H. Yamada, *Chem. Pharm. Bull.* **1994**, 42, 1356–1365.
- [6] F. W. Lichtenthaler, S. Immel, *Tetrahedron: Asymmetry* **1994**, 5, 2045–2060.
- [7] K. Fujita, H. Shimada, K. Ohta, Y. Nogami, K. Nasu, *Angew. Chem.* **1995**, 107, 1783–1784; *Angew. Chem. Int. Ed. Engl.* **1995**, 34, 1621–1622.
- [8] Y. Nogami, K. Fujita, K. Ohta, K. Nasu, H. Shimada, C. Shinohara, T. Koga, *J. Inclusion Phenom. Mol. Recognit. Chem.* **1996**, 25, 53–56.
- [9] P. R. Ashton, C. L. Brown, S. Menzer, S. A. Nepogodiev, J. F. Stoddart, D. J. Williams, *Chem. Eur. J.* **1996**, 2, 580–591.
- [10] F. W. Lichtenthaler, S. Immel, *J. Inclusion Phenom. Mol. Recognit. Chem.* **1996**, 5, 3–16.
- [11] Y. Nogami, K. Nasu, T. Koga, K. Ohta, K. Fujita, S. Immel, H. J. Lindner, G. E. Schmitt, F. W. Lichtenthaler, *Angew. Chem.* **1997**, 109, 1987–1991; *Angew. Chem. Int. Ed. Engl.* **1997**, 36, 1899–1902.
- [12] a) N. Yoshie, H. Hamada, S. Takada, Y. Inoue, *Chem. Lett.* **1993**, 353–356; b) T. Uchiyama, M. Kawamura, T. Urugami, H. Okuno, *Carbohydr. Res.* **1993**, 241, 245–248.
- [13] F. W. Lichtenthaler, S. Immel, *Liebigs Ann. Chem.* **1996**, 27–37.
- [14] S. Immel, G. E. Schmitt, unpublished results.
- [15] a) S. J. Angyal, *Aust. J. Chem.* **1968**, 21, 2737–2746; b) M. K. Dowd, A. D. French, P. J. Reilly, *Carbohydr. Res.* **1994**, 264, 1–19.
- [16] F. W. Lichtenthaler, S. Mondel, *Carbohydr. Res.* **1997**, 303, 293–302.
- [17] D. E. Koshland, Jr., *Angew. Chem.* **1994**, 106, 2368–2372; *Angew. Chem. Int. Ed. Engl.* **1994**, 33, 2375–2378.
- [18] a) E. Fischer, *Ber. Dtsch. Chem. Ges.* **1894**, 27, 2985–2993; b) F. W. Lichtenthaler, *Angew. Chem.* **1994**, 106, 2456–2467; *Angew. Chem. Int. Ed. Engl.* **1994**, 33, 2364–2374.

FULL PAPER

F. W. Lichtenthaler et al.

- [19] C. A. G. Haasnoot, F. A. A. M. DeLeeuw, C. Altona, *Tetrahedron* **1980**, *36*, 2783–2792.
- [20] W. Heiden, G. Moeckel, J. Brickmann, *J. Comput.-Aided Mol. Des.* **1993**, *7*, 503–514.
- [21] a) J. Brickmann, *MOLCAD - MOLEcular Computer Aided Design*, Darmstadt University of Technology, **1996**; *J. Chem. Phys.* **1992**, *89*, 1709–1721; b) J. Brickmann, T. Goetze, W. Heiden, G. Moeckel, S. Reiling, H. Vollhardt, C.-D. Zachmann, *Interactive Visualization of Molecular Scenarios with the MOLCAD/SYBYL Package*, in *Data Visualization in Molecular Science: Tools for Insight and Innovation* (Ed.: J. E. Bowie), Addison–Wesley, Reading, MA **1995**, pp. 83–97.
- [22] M. Teschner, C. Henn, H. Vollhardt, S. Reiling, J. Brickmann, *J. Mol. Graphics* **1994**, *12*, 98–105.
- [23] M. L. Connolly, *J. Appl. Crystallogr.* **1983**, *16*, 548–558.
- [24] a) R. Breslow in *Inclusion Compounds, Vol. 3* (Eds.: J. L. Atwood, J. E. D. Davies, D. D. MacNicol), Academic Press, London, **1984**, pp. 473–508; M. Komiyama, H. Shikigawa in *Comprehensive Supramolecular Chemistry, Vol. 3* (Eds.: J. Szejtli, T. Osa), Pergamon, Oxford, **1996**, pp. 401–422; b) R. Breslow, S. D. Dong, *Chem. Rev.* **1998**, *98*, 1997–2011.
- [25] B. R. Brooks, R. E. Bruccoleri, B. D. Olafson, D. J. States, S. Swaminathan, M. Karplus, “CHARMM: A program for macromolecular energy, minimization, and dynamics calculations” in *J. Comp. Chem.* **1983**, *4*, 187–217.
- [26] S. Reiling, M. Schlenkrich, J. Brickmann, *J. Comput. Chem.* **1996**, *17*, 450–468.
- [27] S. Immel, *MolArch⁺ – MOLEcular ARCHitecture Modeling Program*, Darmstadt University of Technology, **1997**.
- [28] a) D. Cremer, J. A. Pople, *J. Am. Chem. Soc.* **1975**, *97*, 1354–1358; b) G. A. Jeffrey, R. Taylor, *Carbohydr. Res.* **1980**, *81*, 182–183.
- [29] a) H. J. Lindner, M. Kroeker, *PIMM91-Closed Shell PI-SCF-LCAO-MO-Molecular Mechanics Program*, Darmstadt University of Technology, **1996**; b) A. E. Smith, H. J. Lindner, *J. Comput.-Aided Mol. Des.* **1991**, *5*, 235–262.

Received: March 30, 1999 [F 1709]

Inclusion Complexes of Cycloaltrins

S. Immel and K. L. Larsen, *unpublished results*.

The formation of inclusion complexes by the α -^[1] β -^[2] and γ -cycloaltrins^[3] with various *para*-substituted sodium benzoates and the corresponding 1:1 association constants were determined by capillary electrophoresis^[4] according to the protocol previously described for the measurement of stability constants for complexes formed by cyclodextrins of varying ring size.^[5] The electrophoresis capillary was filled with the sodium benzoates and the cycloaltrins were injected as the analyte; the mobility of the macrocycles was monitored as a function of benzoate concentration and the formation of the complexes was detected by UV absorbance (Table 1, *method 1*). Table 1 lists the corresponding $K_{1:1}$ complex formation constants obtained by non-linear regression along with their standard deviations, respectively. For comparison, the association constants between α - and γ -cyclodextrin and the benzoate guest molecules were determined by the same method. In addition, Table 1 lists stability constants for α -, β -, and γ -CD complexes determined by an inverse protocol of the capillary electrophoresis (*method 2*).

For the stabilities of the inclusion complexes formed by the native cyclodextrins – despite some minor discrepancies emerging from the two different methods listed in Table 1 – these data show a clear correlation between the size of the *para*-substituent of the guest benzoate and the association constant of the complex formed. With increasing size of the substituent $F < Cl < Br < I$ the stability of the complexes of the cyclodextrins increases, irrespective of the ring size of the host macrocycle. For β - and γ -cyclodextrin, this also applies to *para-tert*-butyl benzoate, which forms complexes that are more stable than with any of the *para*-halogenated benzoates. In this context, the central cavity of α -cyclodextrin seems to be too small to fully accommodate the *tert*-butyl group, which results in a decreased stability of the complex formed between the smallest of the native cyclodextrins with the sterically most demanding host molecule. The complexes formed by α - and β -cyclodextrin exhibit complex formation constants of similar order of magnitude, whereas the complexes of γ -cyclodextrin are generally significantly weaker than those formed by β -cyclodextrin. The most stable complex, obviously, is formed between β -cyclodextrin and *para-tert*-butyl benzoate.

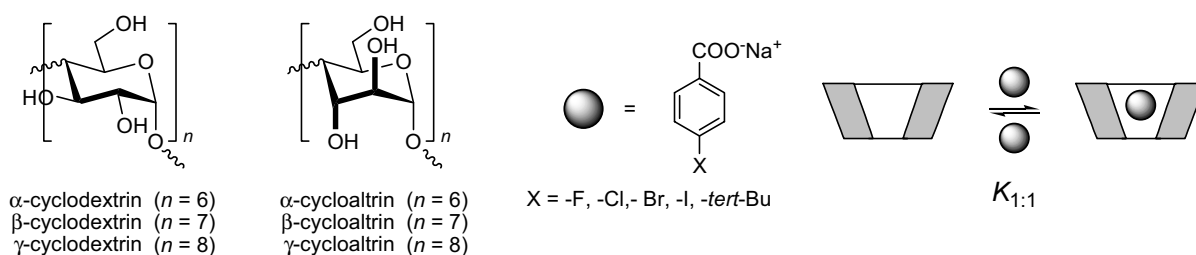


Table 1: Association constants $K_{1:1}$ [l mol^{-1}] between α -, β -, and γ -cycloaltrins or cyclodextrins and various *para*-substituted benzoates (X = -F, -Cl, -Br, -I, and -*tert*-Bu) determined by capillary electrophoresis using different procedures. – *Method 1*: The capillary was filled with buffers containing various concentrations of benzoate derivatives and the various macrocycles was injected as analyte. The mobility of the macrocycles was monitored as a function of benzoate concentration. – *Method 2*: The capillary was filled with buffers containing various concentrations of cyclodextrin and the benzoate derivatives were injected as analyte. The mobility of the benzoate derivatives was monitored as a function of cyclodextrin concentration. – All association constants were obtained by non-linear regression with standard deviations given in parenthesis; “*large*” and “*small*” indicates association constants that are, respectively, too large or too small to be assessed by this method.

host (<i>method 1</i>)	X = -F	X = -Cl	X = -Br	X = -I	X = - <i>tert</i> -Bu
α -cycloaltrin	14.9(0.9)	“ <i>small</i> ”	7.9(1.1)	12.0(0.6)	20.6(1.7)
β -cycloaltrin	14.4(1.3)	11.1(3.4)	10.3(0.6)	9.5(0.8)	16.5(1.6)
γ -cycloaltrin	14.8(2.6)	8.1(0.9)	9.1(1.0)	“ <i>small</i> ”	16.6(1.9)
α -cyclodextrin	21.4(0.8)	“ <i>large</i> ”	“ <i>large</i> ”	“ <i>large</i> ”	102.6(4.5)
γ -cyclodextrin	6.1(0.8)	8.9(1.5)	16.4(2.0)	46.6(7.6)	80.4(4.3)
host (<i>method 2</i>)	X = -F	X = -Cl	X = -Br	X = -I	X = - <i>tert</i> -Bu
α -cyclodextrin	11.9(0.9)	129.3(1.9)	370.2(10.7)	780.4(86.8)	71.7(13.1)
β -cyclodextrin	36.8(3.6)	139.5(9.6)	236.2(7.6)	608.8(20.6)	7304.8(103.9)
γ -cyclodextrin	0.6(2.0)	6.9(1.4)	12.6(1.3)	30.2(1.3)	93.4(1.6)

In contrast to the cyclodextrins, the cycloaltrins display, in all cases, quite low stability constants $K_{1:1}$ ranging only from 8 to 20 l mol^{-1} . There also seems to be no obvious effect of ring size of the cycloaltrin host. From the data presented in Table 1, it can be concluded that the most stable complexes are formed with *para-tert*-butyl benzoate, the same guest molecule that forms the most stable complexes with the cyclodextrins. However, curiously the weakest complex former of the *para*-halogenated benzoates (*para*-fluoro benzoate) with the native CD seems to be the best for the cycloaltrins, and again no effect of cycloaltrin macrocycle size can be detected. Yet, it is noteworthy, that with the *para*-fluoro, *para*-chloro, and *para*-bromo benzoates, the cycloaltrin complexes are more stable or comparable to the complexes formed by γ -cyclodextrin.

In total, the data presented seems to suggest that the inclusion complexes formed by the cycloaltrins are based on weak unspecific interactions. The selectivity of the cycloaltrins with respect to the size and shape of the guest molecules is less pronounced than for the cyclodextrins of the same ring size. This may be interpreted in terms of the increased conformational flexibility of the cycloaltrins, which seem to

be able to accommodate their shape towards a greater range of guest molecules than the cyclodextrins are. On the other hand, the rather low absolute association constants also reflect a significant entropy penalty to be paid upon the formation of inclusion complexes by the cycloaltrins.

All the data presented suggests two entirely different mechanisms for the formation of inclusion complexes: whereas the cyclodextrins follow the rather rigid *lock-and-key*-type mechanism of complex formation, the cycloaltrins are of significantly higher flexibility. The formation of complexes by cycloaltrins is best described by the flexible *induced-fit* mechanism which implies considerable geometrical flexibility of the host, along with its conformational adaptation towards potential guest molecules. Further evidence for this hypothesis is derived from the formation of inclusion complexes by mono-altro- β -cycloaltrin^[6] described in the next Chapter of this work.

References

- [1] Y. Nogami, K. Nasu, T. Koga, K. Ohta, K. Fujita, S. Immel, H. J. Lindner, G. E. Schmitt, and F. W. Lichtenthaler, *Angew. Chem., Int. Ed. Engl.* **1997**, *36*, 1899-1902; S. Immel, K. Fujita, and F. W. Lichtenthaler, *Chem. Eur. J.* **1999**, *5*, 3185-3192.
- [2] K. Fujita, H. Shimada, K. Ohta, Y. Nogami, K. Nasu, and T. Koga, *Angew. Chem., Int. Ed. Engl.* **1995**, *34*, 1621-1622.
- [3] Y. Nogami, K. Fujita, K. Ohta, K. Nasu, H. Shimada, C. Shinohara, and T. Koga, *J. Inclusion Phenom. Mol. Recognit. Chem.* **1996**, *25*, 57-60.
- [4] K. L. Larsen, F. Mathiesen, and W. Zimmermann, *Carbohydr. Res.* **1997**, *298*, 59-63.
- [5] K. L. Larsen, T. Endo, H. Ueda, and W. Zimmermann, *Carbohydr. Res.* **1998**, *309*, 153-159.
- [6] K. Fujita, W.-H. Chen, D.-Q. Yuan, Y. Nogami, T. Koga, T. Fujioka, K. Mihashi, S. Immel, and F. W. Lichtenthaler, *Tetrahedron: Asymmetry* **1999**, *10*, 1689-1696.

